DISCRETE AND CONTINUOUS
DYNAMICAL SYSTEMS SERIES B

doi:10.3934/dcdsb.2021166

ANALYSIS OF STATIONARY PATTERNS ARISING FROM A TIME-DISCRETE METAPOPULATION MODEL WITH NONLOCAL COMPETITION

Ozgur Aydogmus*

Department of Economics, Social Sciences University of Ankara
Ulus-Ankara, Turkey

Yun Kang

Sciences and Mathematics Faculty
College of Integrative Sciences and Arts, Arizona State University
Mesa, AZ 85212, USA

(Communicated by Frithjof Lutscher)

Abstract. The paper studies the pattern formation dynamics of a discrete in time and space model with nonlocal resource competition and dispersal. Our model is generalized from the metapopulation model proposed by Doebeli and Killingback [2003. Theor. Popul. Biol. 64, 397-416] in which competition for resources occurs only between neighboring populations. Our study uses symmetric discrete probability kernels to model nonlocal interaction and dispersal. A linear stability analysis of the model shows that solutions to this equation exhibits pattern formation when the dispersal rate is sufficiently small and the discrete interaction kernel satisfies certain conditions. Moreover, a weakly nonlinear analysis is used to approximate stationary patterns arising from the model. Numerical solutions to the model and the approximations obtained through the weakly nonlinear analysis are compared.

1. **Introduction.** The role of spatial structure on ecological processes has been the central theme of many studies (see, e.g. [8, 12, 19, 20, 21, 26, 33, 35]). Population fluctuations and geographical patterns of population abundances are among the most important topics in ecological theory [11, 23, 27]. A stable spatially homogenous equilibrium state of an ecosystem can be destabilized via the Turing mechanism [41] when there are multiple species interacting (see e.g. [33]). These diffusion-driven instabilities have been observed in many systems including models which are continuous in both time and space [16, 17, 28, 33], discrete in space and continuous in time [9], continuous in space and discrete in time [34], or discrete in time and space [36]. In addition to diffusion, other nonlocal ecological interactions

2020 *Mathematics Subject Classification.* Primary: 39A99, 92D40; Secondary: 92C15.

Key words and phrases. Nonlocal coupling, metapopulation, pattern formation, multiscale perturbation, weakly nonlinear analysis.

This research of YK is partially funded by the NSF-DMS (Award Number 1716802); the NSF-IOS/DMS (Award Number 1558127); DARPA-SBIR 2016.2 SB162-005; and the James S. McDonnell Foundation 21st Century Science Initiative in Studying Complex Systems Scholar Award (UHC Scholar Award 220020472).

* Corresponding author.

(e.g., competition for resources) are considered to be another important mechanism for generating spatial patterns [2, 4, 5, 7, 11, 18].

Doebeli and Killingback in [11] considered the coupling between the nearest neighboring habitat patches with wrap around boundary conditions to study the effects of quasi-local ecological interactions and simple dispersal. They assumed that the growth of each local population is governed by a difference equation and that the coupling occurs mainly through quasi-local interactions. In their model, the reproductive dynamics of a local population in a given patch depends not only on the population density in that patch but also on the population abundances in the nearest neighboring patches.

Motivated by the work of Doebeli and Killingback [11], we consider a generalized discrete-time metapopulation model in both one- and two-dimensional spatial habitats. Throughout the paper, we assume that both dispersal and nonlocal interactions are modeled by discrete probability kernels describing the range and strength of the ecological forces. These kernels are useful in modeling the competition for common resources such as food, energy, or water that are basic requirements for the growth of any population. Examples of such competitions between populations living in neighboring spatial locations include foraging in ant colonies [6] or dunnocks [10]. Another ecologically meaningful example of such competition is the consumption of diffusible resources like water needed by plants [22, 25, 32].

In this paper, our aim is threefold. Firstly, we take nonlocal rather than quasi-local interactions into account, and we model these interactions using discrete probability distributions as done in [4]. Our assumption is more relaxed than the quasi-local interactions assumptions in [11]. This relaxation reflects that the strength of the ecological interactions (including dispersal) impinging on a population in a patch is a function of the neighboring population densities as well as of their spatial distance, with more distant patches having a smaller impact.

Secondly, we perform a linear stability analysis of the model taking nonlocal interactions into account. Due to the assumption of quasi-local interactions in [11], the linearization of the metapopulation model leads to a Toeplitz matrix. Hence, Doebelli and Killinback numerically computed the eigenvalues of the system. Instead, we employ discrete Fourier series (DFS) [38] to perform a linear analysis of the metapopulation model coupled through nonlocal interactions. This analysis allows us to relate the conditions obtained in [11] and other authors (see, e.g., [7, 18]) to observe pattern formation.

Lastly, we employ the classical Stuart-Landau (S-L) theory [39] to study the effect of nonlocal interactions near the stability boundary. Weakly nonlinear analysis of patterns arising from partial differential equations and other continuum models have been widely studied in the literature (see, e.g., [2, 13, 16, 33, 40]). The method was employed to analyze patterns arising from integro-difference equations and continuous-time metapopulations only recently [4, 5]. To our knowledge, this theory has never been employed to study discrete-in-time metapopulations consisting several local habitat patches. By using these results, we obtain first-order approximations to stable patterns in 1- and 2-dimensional habitats following [17].

The paper is organized as follows: In Section 2, we introduce the notations of the paper and generalize the metapopulation model proposed in [11] by incorporating nonlocal dispersal and competition. In Section 3, we perform a linear stability analysis of the model near its spatially homogenous solution and find conditions to observe pattern formation. In Section 4, four specific examples are presented. We

obtain cubic S-L equations for our metapopulation model in Section 5. In addition, we perform numerical simulations of stationary patterns arising from the examples and their first-order approximations. In Section 6, we conclude the paper.

2. **The model.** In this section, we introduce the metapopulation dynamics proposed in [11]. Then we define the convolution operator on 1- and 2-dimensional lattices and use it to reformulate this model. Such a reformulation will be useful in generalizing and subsequently analyzing the model.

We first consider an environment S having $Q_1 \times Q_2$ patches with wrap around boundary conditions where Q_1 and Q_2 are integers. In particular, a metapopulation consisting of several distinct populations is shown in Figure 1. In the figure, each square cell represents a patch in which a group of spatially separated populations of the same species lives. It is assumed that there exists a spatially homogeneous sub-population in each patch and these sub-populations interact at some level.

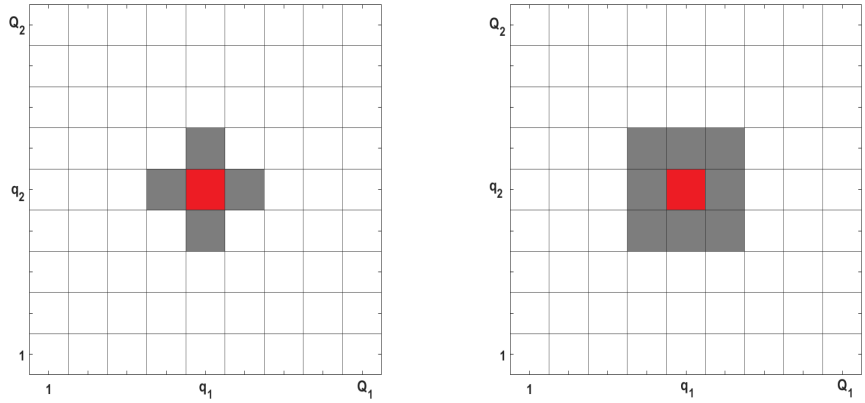

(a) von Neumann neighborhood (b) Moore neighborhood

FIGURE 1. The patchy environment S and neighborhoods of a patch $q = (q_1, q_2)$. In Panels (a) and (b), von Neumann and Moore neighborhoods of patch (q_1, q_2) (colored in red) are determined by patches colored in gray, respectively.

A map is used to describe the population dynamics at a patch $q = (q_1, q_2) \in S = \{1, 2, \cdots, Q_1\} \times \{1, 2, \cdots, Q_2\}$ in [11]. To write the difference equation in a compact form, we need to specify how these sub-populations interact. Recall two major neighborhoods used to study the effects of nearest neighbor competition and dispersal in metapopulation models. The von Neumann neighborhood of radius r of site q is given as follows:

$$N_N^q(r) = \{(p_1, p_2) : 0 < \langle |p_1 - q_1| \rangle_{Q_1} + \langle |p_2 - q_2| \rangle_{Q_2} \leq p\}$$

where $< q >_Q = q$ Modulo Q. Another commonly used neighborhood is the Moore neighborhood of radius r defined as follows:

$$N_M^q(r) = \{(p_1, p_2) : 0 < \langle |p_1 - q_1| \rangle_{Q_1} \leq r, 0 < \langle |p_2 - q_2| \rangle_{Q_2} \leq r\}.$$

In Figures 1 (a) and (b), von Neuman and Moore neighborhoods of patch $q = (q_1, q_2)$ of radius 1 (i.e., $N_N^q(1)$ and $N_M^q(1)$) are illustrated, respectively.

By taking $Q_2 = 1$, both of the above given neighborhoods reduce to the following neighborhood in a 1 dimensional habitat:

$$N_1^q(r) = \{p : 0 < \langle |p - q| \rangle_{Q_1} \leq r\}.$$

Remark that all of the above-given neighborhoods exclude self-interaction. In [11], it was assumed that the per capita reproductive output is of Beverton–Holt type:

$$x_q'(t) = \frac{\lambda x_q(t)}{1 + \tilde{a}\left[x_q + \alpha \sum_{p \in N_n^q(1)} x_p(t)\right]} \tag{1}$$

where $x_q(t)$ is the local population size in patch q at the start of year t and $x_q'(t)$ is the local population size in patch q after reproduction. Here the summation in the denominator models the relative competitive impact of individuals from the neighboring patches on reproduction in patch q for any neighborhood $N_n^q(1)$, $n = 1, N, M$. The parameter λ in (1) describes the maximal per capita reproductive output attained. In the absence of competition, the parameter $\tilde{a}$ is a measure of the impact of the population size on the reproduction in patch q.

To complete the metapopulation dynamics, it was assumed in [11] that the reproduction is followed by a passive dispersal of a constant fraction of the local populations, which is distributed evenly between the neighboring patches. The dispersal operator is given by

$$x_q(t+1) = (1 - \delta)x_q'(t) + \frac{\delta}{s_n} \sum_{p \in N_n^q(1)} x_p'(t) \tag{2}$$

where δ is the fraction of dispersers, $x_q'(t)$ is the size of the population in year t after reproduction but before dispersal, and s_n is the cardinality of the neighborhood $|N_n^q(1)|$.

We would like to note that many discrete-time spatial population models have two phases: The first phase describes the growth of the population as in (1). The second phase describes the dispersal of the individuals from site q to its neighboring sites in $N^q(1)$ as in (2).

The above-given model taking quasi-local (or nearest neighbor) interactions into account has been analyzed in [11]. Computational results regarding the magnitudes of the eigenvalues of the linearized system corresponding to (1) and (2) were obtained when the interactions and dispersal are limited only to nearest neighbors, i.e., $r = 1$.

We define the convolution of matrices in the following lines to reformulate the growth-dispersal model (1-2). Discrete convolution operator of two matrices $\mathbf{x}$ and $\mathbf{y}$ on a two-dimensional lattice is given as follows:

$$(\mathbf{x} * \mathbf{y})_k = \sum_{m=1}^{Q_1} \sum_{n=1}^{Q_2} x_{m,n} y_{<m-k_1>_{Q_1}, <n-k_2>_{Q_2}}. \tag{3}$$

Note that $\mathbf{x} * \mathbf{y}$ is a matrix of size $Q_1 \times Q_2$. In addition, when $Q_2 = 1$, this operator reduces to convolution operator in 1-dimensional habitat.

Now we can reformulate the model (1-2) so that it takes the more general interaction and dispersal ranges and weights into account. Consider two symmetric

discrete probability kernels $\mathbf{d}$ and $\mathbf{c}$ used to model nonlocal dispersal and interactions. By considering such kernels, we relax the assumption that each site in the habitat interacts only with its nearest neighbors. For these two kernels $\mathbf{d}$ and $\mathbf{c}$, we only assume that they are symmetric. Using the interaction kernel $\mathbf{c}$, the growth equation taking nonlocal interactions into account can be written as follows:

$$x'_q(t) = \frac{\lambda x_q(t)}{1 + a(\mathbf{c} * \mathbf{x})_q}. \tag{4}$$

Besides, one can also write the dispersal equation as the convolution of the dispersal kernel and the nonlinear growth function as

$$x_q(t+1) = \delta(\mathbf{d} * \mathbf{x}')_q + (1-\delta)x'_q(t). \tag{5}$$

The quasi-local interaction kernel numerically studied in [11] can be taken as a specific example for the interaction kernel. This kernel is given as follows:

$$\mathscr{c}_q^n = \begin{cases} (1+s_n\alpha)^{-1}, & \text{for } q = 0 \\ \alpha(1+s_n\alpha)^{-1}, & \text{for } q \in N_n^0(1) \\ 0, & \text{elsewhere.} \end{cases} \tag{6}$$

for $n = 1, N, M$. Here the interaction term in (1) can be written as the convolution of two matrices $\mathbf{x}$ and $\boldsymbol{\mathscr{c}}^n = (\mathscr{c}_q^n)_{q\in S}$. For $a = \tilde{a}(1+s_n\alpha)$, the right hand sides of growth terms (1) and (4) are equal. When $\mathbf{d}$ is taken as the uniform distribution on $N_n^q(1)$, the right hand sides of dispersal equations (2) and (5) are also equal. Hence the model (1-2) can be written by using convolutions as in (4-5).

Here (4) and (5) together describe the dynamics of several sub-populations dispersing to neighborhood patches and competing for the common resources with the residents of other patches. Here the foraging and dispersal ranges are determined by the supports of the discrete probability distributions $\mathbf{c}$ and $\mathbf{d}$, respectively. The dispersal rate or probability δ, on the other hand, describes the average proportion of individuals that are expected to disperse to other sites.

Lastly, note that the Coupled Map Lattice (CML) described by (4) and (5) has a spatially homogeneous state $\mathbf{e} = (\frac{\lambda-1}{a})_{q\in S}$ where $\frac{\lambda-1}{a}$ is the stable equilibrium of the classical Beverton-Holt equation for $\lambda > 1$ and $a > 0$.

3. **Linear analysis using discrete Fourier series.** In this section, we aim to find an explicit expression for the eigenvalues of linearized problem described by (4-5). Such an expression will be useful to study how nonlocal interaction kernel $\mathbf{c}$ and system parameters, including the dispersal rate δ, affect the stability of space-homogeneous solution $\mathbf{e}$.

It is known that the nearest neighbor (or quasi-local) competition destabilizes the space-homogeneous solution to (1-2) [11]. They obtained this result by analyzing the $|S|$ dimensional system of difference equations (1-2) when the nearest neighbor (or quasi-local) interactions take place. One needs the following properties of the discrete Fourier series (DFS) to find an analytical expression of the eigenvalues for the linearization of the model (4-5), taking nonlocal interactions into account.

Discrete Fourier series (DFS) of a matrix $\mathbf{x} = (x_{m,n})_{(m,n)\in S}$ is denoted by $\mathscr{F}\mathbf{x}$ and k^{th} entry of which is given by

$$(\mathscr{F}\mathbf{x})_k = \sum_{(m,n)\in S} x_{m,n} e^{-2j\pi k_1 m/Q_1} e^{-2j\pi k_2 n/Q_2} \tag{7}$$

for any $k = (k_1, k_2) \in S$ [31, 38]. Here we would like to remark that the discrete convolution theorem also holds in 2-D lattices and is given by the following equality:

$$(\mathscr{F}\mathbf{x} * \mathbf{y})_k = (\mathscr{F}\mathbf{x})_k \cdot (\mathscr{F}\mathbf{y})_k \tag{8}$$

where $\cdot$ represents the component-wise multiplication or Hadamard product of two matrices [31, 38]. Note also that the above given properties of the matrices are also valid in a 1-D habitat. For a review of these results in a 1-D patchy environment, one can consult [4, Section 2.1].

We linearize the CML by using the first order expansion $\mathbf{x}(t) = \mathbf{e} + \varepsilon\check{\mathbf{x}}\rho^t$, where $\check{\mathbf{x}}$ is a time-independent matrix denoting a spatial perturbation term. Substituting this ansatz to equation (4), we obtain $G[\check{\mathbf{x}}, \mathbf{c} * \check{\mathbf{x}}] = \check{\mathbf{x}} + \frac{1-\lambda}{\lambda}\mathbf{c} * \check{\mathbf{x}}$ at the level $O(\varepsilon)$. Hence (5) takes the following form:

$$\rho\check{\mathbf{x}} = \delta\mathbf{d} * G[\check{\mathbf{x}}, \mathbf{c} * \check{\mathbf{x}}] + (1-\delta)G[\check{\mathbf{x}}, \mathbf{c} * \check{\mathbf{x}}].$$

Taking the DFS of both sides in the above equation and using the convolution theorem (8) lead us to the following eigenvalues:

$$\rho_k(\delta) = \lambda^{-1}\big(\delta(D_k - 1) + 1\big)(\lambda + C_k - \lambda C_k) \tag{9}$$

where $\mathbf{C} = (C_k)_{k\in S}$ and $\mathbf{D} = (D_k)_{k\in S}$ are the DFS of the competition and dispersal kernels $\mathbf{c}$ and $\mathbf{d}$, respectively. In particular, we have $C_k = (\mathscr{F}\mathbf{c})_k$ and $D_k = (\mathscr{F}\mathbf{d})_k$. Since both of these kernels are assumed to be symmetric discrete probability distributions, the DFS of them take real values between -1 and 1. If there is no spatial effect, we have the eigenvalue $\rho = 1/\lambda$ that is less than 1 if $\lambda > 1$. Hence, $\mathbf{e}$ is the stable equilibrium of the CML for any $\lambda > 1$.

First, we consider the eigenvalues (9) in the absence of spatial dispersal, i.e., $\delta = 0$. Such a simplification allows us to identify the properties of the interaction kernel $\mathbf{c}$ for which $\mathbf{e}$ looses its stability. When $\delta = 0$, the eigenvalues are given as follows:

$$\rho_k(0) = \lambda^{-1}(\lambda + C_k - \lambda C_k).$$

Note that $\rho_k(0)$ is always non-negative for any $k \in S$ and $\lambda > 1$. Then, $\mathbf{e}$ is unstable if the magnitude of an eigenvalue $\rho_k(0)$ is larger than 1. One can easily conclude that $\rho_k(0) > 1$ for any $\lambda > 1$ if and only if C_k is negative for some $k \in S$.

This result can be considered as a more general version of the stability result obtained in [11]. In particular, they considered interaction kernel $\boldsymbol{\mathscr{c}}^1$ given by (6) in a 1-dimensional habitat. When there is no dispersal and the number of the patches in the habitat is even, they showed that $\mathbf{e}$ loses its stability if $\alpha > \frac{1}{2}$.

Here we can get the same result by taking $\mathbf{c} = \boldsymbol{\mathscr{c}}^1$. Note that the DFS of competition kernel $\boldsymbol{\mathscr{c}}^1$ is given by $\mathscr{C}^1_k = (1+2\alpha)^{-1}\big(1 + 2\alpha\cos(2\pi k/N)\big)$. Note also that the smallest entry in $\boldsymbol{\mathscr{C}}^1$ is $\mathscr{C}^1_{N/2} = (1+2\alpha)^{-1}\big(1-2\alpha\big)$. Hence, $\mathscr{C}^1_k$ is negative for at least one $k \in S$ if and only if $\alpha > \frac{1}{2}$. In [11], a similar analysis was performed for $\boldsymbol{\mathscr{c}}^N$ given by (6) in a 2-dimensional habitat and it was shown that $\mathbf{e}$ loses its stability if $\alpha > \frac{1}{4}$. It is easy to show that this condition is also equivalent to the condition that $\mathscr{C}^N_k$ is negative for some $k \in S$.

It was found in [11] that quasi-local competition destabilizes the spatially uniform equilibrium in the absence of dispersal provided that the competitive impact of the neighboring patches on the reproduction in a patch is sufficiently large. This statement for more general nonlocal interactions takes the following mathematical form: if the DFS of the interaction kernel C_k is negative for some $k \in S$ then the spatially uniform equilibrium is unstable in the absence of dispersal. Note that the

latter statement is known to hold for many other models taking nonlocal interactions into account (see, e.g., [2, 3, 4, 5, 18]).

In the remainder of this paper, we assume that C_k is negative for some $k \in S$. This implies that $\rho_k(0) > 1$ for some $k \in S$. Hence $\rho_k(\delta)$ is larger than 1 for δ small enough by continuity. The critical dispersal rate $\delta_0 \in (0, 1)$ can be calculated by solving the following root finding problem:

$$\max_{k \in S} \{\rho_k(\delta) - 1\} = 0 \tag{10}$$

The argument of this maximization problem is denoted by k^c and called the most unstable wavenumber. Since $\delta(D_k - 1) + 1 \leq 1$ for any $\delta \in [0, 1]$, the magnitude of the eigenvalues $\rho(\delta)$ decreases as δ increases. This implies that $\rho(\delta) > 1$ for any $\delta < \delta_0$. As a result, we conclude that increasing the dispersal rate flattens the spatial heterogeneity.

4. **Examples.** In this section, we provide four numerical examples with different kernels in 1-D and 2-D habitats. We compute their critical dispersal rates and the most critical wavenumbers. For all our examples presented in this section, we fix the following parameter values: $a = 1$, $\lambda = 2$ and $Q_1 = 20$.

Recall that the neighborhoods $N_n^q(r)$ for $n = 1, N, M$ defined in Section 2 do not contain the point q. Here, we define the extended neighborhoods $\mathcal{N}_n^q(r) = N_n^q(r) \cup \{q\}$ that will be useful in describing competition kernels $\mathbf{c}$ in the following examples.

To illustrate the spatially uniform equilibrium $\mathbf{e}$ loses its stability for some dispersal rates in a 1-dimensional habitat (i.e., $Q_2 = 1$), we take the following examples into account:

E1: First, we consider quasi-local (nearest neighbor) interactions and dispersal. We take the dispersal kernel $\mathbf{d}$ as the uniform distribution in $N_1^q(1)$ and the competition kernel $\mathbf{c}$ as the uniform distribution in $\mathcal{N}_1^q(1)$. With these kernels, we have the critical dispersal rate $\delta_0 = 0.071428$ along with the most unstable wavenumber $k^c = 10 = (10, 1)$ (see Figure 2(a)). Patterns arising from the CML with the above-given kernels and dispersal rate $\delta = 0.0714$ are illustrated in Figure 3(a).

E2: Second, we consider next to nearest neighbor (or nonlocal) interaction and dispersal in a 1-dimensional habitat. Hence, we take the dispersal kernel $\mathbf{d}$ as the uniform distribution in $N_1^q(2)$ and the competition kernel $\mathbf{c}$ as the uniform distribution in $\mathcal{N}_1^q(2)$. In this case, we have $\delta_0 = 0.070563$ along with the most unstable wavenumbers $k_1^c = 6 = (6, 1)$ and $k_2^c = 14 = (14, 1)$ (see Figure 2(b)). Patterns arising from the CML with the above-given kernels and dispersal rate $\delta = 0.0705$ are illustrated in Figure 4(a).

In a 2-dimensional habitat with $Q_2 = 20$, we considered instabilities arising from the CML using both von Neumann and Moore neighborhoods as follows:

E3: Here, we use a von Neumann neighborhood in a 2-dimensional habitat (see, Figure 1(a)). In particular, we consider competition and dispersal kernels as uniform distributions on $\mathcal{N}_N^q(1)$ and $N_N^q(1)$, respectively. Then, we have the critical dispersal rate $\delta_0 = 0.11538$ along with the most unstable wavenumber $k^c = (10, 10)$ that is marked in Figure 2(c). Patterns arising from the CML with the above-given kernels and dispersal rate $\delta = 0.115$ are illustrated in

Figure 3(c).

E4: When using a Moore neighborhood (see, Figure 1(b)), we have competition and dispersal kernels as uniform distributions on the sets $\mathcal{N}_N^q(1)$ and $N_N^q(1)$, respectively. In this case, $\delta_0 = 0.095238$ along with two the most unstable wavenumbers $k_1^c = (10, 20)$ and $k_2^c = (20, 10)$ that are marked in Figure 2(d). Patterns arising from the CML with the above-given kernels and dispersal rate $\delta = 0.095$ are illustrated in Figure 5(a).

Here, we remark that the critical dispersal rate δ_0 for each example is found by numerically solving the root-finding problem (10). The critical wavenumber k^c is equal to $k \in S$ satisfying $\rho_k(\delta_0) \geq 1$, i.e., it is the argument of the maximization problem $\max_{k\in S}\{\rho_k(\delta) - 1\}$ near δ_0. Hence, if there are multiple arguments of this problem, all of them are taken as the most unstable wavenumbers.

In Figure 2, we plot the dispersion relations for the above-given examples **E1-4**. For the examples in 1 dimensional habitat we used bar graphs to show the eigenvalue(s) having the most unstable wavenumber takes values larger than 1 for $\delta = 0.06 < \delta_0$ (see Figures 2(a) and 2(b)). Figures 2(c) and 2(d) illustrate the dispersion relations for examples **E3** and **E4** at δ_0 and the most unstable wavenumbers are marked in these figures.

Note that each of the above-given examples falls into one of the following categories: (i) a single critical wavenumber as in **E1** and **E3**, (ii) a pair of complex conjugate wavenumbers as in **E2**, and (iii) two independent wavenumber as in **E4**. For the examples given in this section, different types of patterns near the stability boundaries will be illustrated in the following section. In addition, we approximate these patterns (stationary solutions to CML) near the stability boundaries using the eigenvalues and eigenvectors corresponding to the most unstable wavenumbers. In particular, we perform a weakly nonlinear analysis of the CML which heavily depends on these critical wavenumbers. Analyses regarding cases (i), (ii) and (iii) are given in Sections 5.1.1, 5.1.2 and 5.2, and technical details of the nonlinear analyses regarding these cases are deferred to Appendices A.1, A.2 and A.3, respectively.

5. Weakly nonlinear analysis.

The linear stability analysis is a useful tool to examine the effects of the parameters and interaction kernels on the stability of the system, but it is only valid for small-time and infinitesimal perturbations. In the long run, nonlinear terms affect the growth of unstable modes. Hence, in the following lines, we consider the CML model (4-5) and obtain the Stuart-Landau (S-L) equations [39] to approximate the stationary patterns in 1-D and 2-D habitats.

We are interested in the stability of the homogenous solution $\mathbf{e}$ near the critical dispersal rate δ_0 with periodic boundary conditions. We aim to approximate the solution to (5) by using the steady-state solutions to the amplitude equations. To find these equations, consider a perturbation of the bifurcation parameter δ as follows:

$$\delta = \delta_0 + \varepsilon^2 \mu \tag{11}$$

for $0 < \varepsilon \ll 1$ and $\mu = \pm 1$. Here μ determines the direction of the deviation from the critical nonlocal dispersal rate δ_0. In Section 3, we showed that $\mathbf{e}$ might be unstable for $\mu = -1$ using the linear stability analysis.

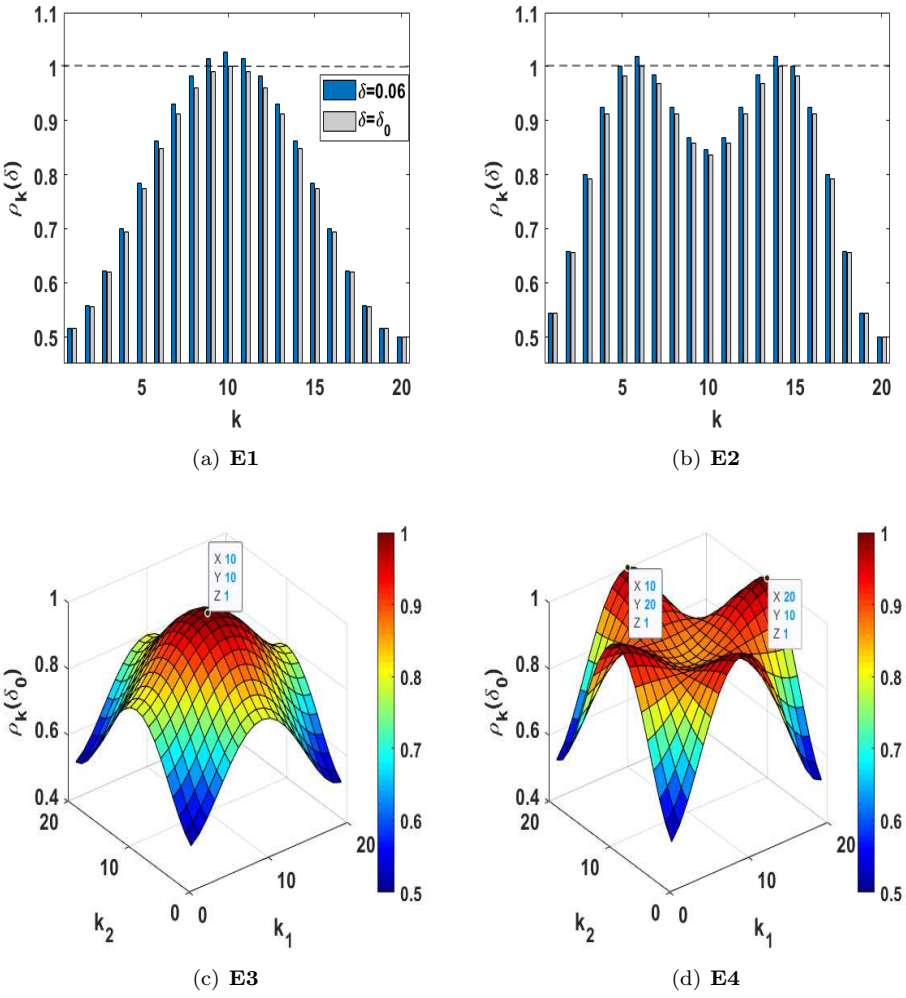

(a) **E1** (b) **E2**

(c) **E3** (d) **E4**

FIGURE 2. Dispersion relations for the examples **E1-4**.

Let δ_0 be the critical dispersal rate for which we have $\rho_{k^c}(\delta_0) = 1$ for all k^c satisfying (10). The solution to the linearized CML around $\mathbf{e}$ and near critical dispersal rate δ_0 is given as follows:

$$\mathbf{y}_t \propto \sum_{k^c} \mathbf{w}_{k^c} \cdot \big(\rho_{k^c}(\delta)\big)^t \tag{12}$$

where $\mathbf{w}_{k^c} = \big(w_{k^c}[q_1, q_2]\big)$ is a matrix of size $Q_1 \times Q_2$ with $w_{k^c}[q_1, q_2] = e^{j2\pi k_1^c q_1/Q_1} e^{j2\pi k_2^c q_2/Q_2}$. We remark that $\{\mathbf{w}_k | k \in S\}$ is an orthogonal basis of the vector space $\mathbb{R}^{Q_1 \times Q_2}$ which follows from the discussion in [38, p. 104].

Expanding the eigenvalue $\rho_{k^c}(\delta)$ in power series leads to

$$\rho_{k^c}(\delta) = 1 + \nu\varepsilon^2(D_{k^c} - 1)(1 - \frac{\lambda - 1}{\lambda} C_{k^c}) + O(\varepsilon^4)$$

where we used equality (9) to obtain $d\rho/d\delta$. By substituting this expansion to a summand of solution (12), one obtains

$$\begin{aligned}\mathbf{w}_{k^c}\big(\rho_{k^c}(\delta)\big)^t &= \mathbf{w}_{k^c}e^{t\log(1+\nu\varepsilon^2 d\rho/d\delta)}\\ &\approx \mathbf{w}_{k^c}e^{t\nu\varepsilon^2 d\rho/d\delta}\\ &= A(\varepsilon^2 t)\mathbf{w}_{k^c}.\end{aligned}$$

Here amplitude A is a function of the slow time $\tau := \varepsilon^2 t$. We consider the fast- and slow-time scales t and τ together in our analysis. Following [24], we incorporate the slow-time scale τ into the problem by assuming the solution has an expansion of the form

$$\mathbf{x}_t = \mathbf{e} + \varepsilon\mathbf{x}_1(t,\tau) + \varepsilon^2\mathbf{x}_2(t,\tau) + \cdots. \tag{13}$$

Notice that $\mathbf{x}_1(t,\tau) = \mathbf{y}_t = \sum_i A_i(\tau)\mathbf{w}_{k_i^c}$. This implies that the complexity of solutions increases as the multiplicity of the eigenvalue increases. Since the CML also contains the term $\mathbf{x}_{t+1}$, we expand this term following [24] as follows:

$$\begin{aligned}\mathbf{x}_{t+1} &= \mathbf{x}(t+1,\tau+\varepsilon^2,Q)\\ &= \mathbf{e} + \varepsilon\mathbf{x}_1(t+1,\tau) + \varepsilon^2\mathbf{x}_2(t+1,\tau) + \varepsilon^3\partial_\tau\mathbf{x}_1(t+1,\tau) + O(\varepsilon^4).\end{aligned} \tag{14}$$

$\mathbf{x}_2$ in (13) will be determined in the following sections depending on the multiplicity of the most unstable eigenvalue.

5.1. **Stuart-Landau equations for a single amplitude function.** In this section, we find Stuart-Landau (S-L) equations for a single-amplitude function $A(\tau)$. Categories (i) and (ii) (see Section 4) will be examined in this subsection. The former one is represented by our examples **E1** and **E3** where we have a single eigenvalue corresponding to the most unstable wavenumber (see Figures 2(a) and 2(c)). The latter category is represented by **E2** for which we have two complex conjugate the most unstable wavenumbers (see Figure 2(b)). In the following lines we discuss these two cases in detail.

5.1.1. *S-L equations for a single critical wavenumber.* In this subsection, we assume that the largest eigenvalue is simple as in examples **E1** and **E3**. In this case, we have the first order solution

$$x_1 = A(\tau)\mathbf{w}_{k^c},$$

where the amplitude function $A(\tau)$ satisfies the following S-L equation:

$$\frac{dA}{d\tau} = \mu\psi A + \phi A^3. \tag{15}$$

The details regarding the derivation of (15) and explicit expressions for the parameters ϕ and ψ are given in Appendix A.1. Since coefficients ϕ and ψ of S-L equation (15) are real, the amplitude A can be taken as a real function provided that the initial amplitude $A(0)$ is real.

Steady state solutions of equation (15) are given by

$$A_0 = 0 \text{ and } A_\infty^\pm = \pm\sqrt{-\mu\psi/\phi}. \tag{16}$$

The linear stability analysis of (15) suggests that the solution 0 is stable whenever $\mu\psi < 0$. We can observe that $\psi < 0$ from equality (21). Thus, we can conclude that the steady state solution A_0 (or $\mathbf{e}$) is unstable for $\mu = -1$ and stable for $\mu = 1$. This

result is consistent with the results of the linear analysis in Section 3. If $\phi < 0$, $A_\infty^\pm$ takes real values for $\mu = -1$. Thus we have the following result to approximate the stationary patterns arising from the CML.

Theorem 5.1. *Suppose that $\mu = -1$ and $\varepsilon > 0$ is small enough so that the uniform steady-state $\mathbf{e}$ is unstable to modes corresponding only to the eigenvalue k^c. If $\phi < 0$, an approximation to the emerging solution to CML is given as follows:*

$$\mathbf{x} = \mathbf{e} + \varepsilon A_\infty^\pm \mathbf{w}_k + O(\varepsilon^2),$$

where $A_\infty^\pm$ are as given in (16).

To verify Theorem 5.1 numerically, we consider examples **E1** and **E3** having a single critical eigenvalue. A solution to the CML with parameters given in **E1** and a random initial datum is shown in Panel (a) of Figure 3, while approximation to this solution is shown in Panel (b) of Figure 3. Here $\varepsilon = 0.0053$ and it is verified that the error in predicting the amplitude is of order ε^2. In addition, the equilibria of the S-L equation are given by $A_\infty^\pm = \pm 4.0988$. Hence, the maximum norm of the difference between the stationary solution and its approximation is found as follows: $\|\mathbf{x} - \mathbf{e} - \varepsilon A_\infty^+ \mathbf{w}_{k^c}\|_\infty = .00019$ where $k^c = 10$.

For the second example **E3**, we also have only one critical eigenvalue. Similarly, stationary patterns in 2-D habitat arising from the CML with a random initial datum and its predicted equilibrium solution to first order are shown in Panels (c) and (d) of Figure 3, respectively. In this case, $\varepsilon = 0.0196$ and it is verified that the error in predicting the amplitude is of order ε^2. In addition, the equilibria of the S-L equation are given by $A_\infty^\pm = \pm 3.5187$. The maximum norm of the difference between the stationary solution and its approximation is given as follows: $\|\mathbf{x} - \mathbf{e} - \varepsilon A_\infty^- \mathbf{w}_{k^c}\|_\infty = .039$ where $k^c = (10, 10)$. Hence, we can conclude that the predicted solution shows a good agreement with the numerical solution of the CML.

5.1.2. *S-L equations for a pair of complex conjugate critical wavenumbers.* As in example **E2**, there may be two complex conjugate eigenvalues. In this case we have the first-order solution

$$\mathbf{x}_1 = \tilde{A}(\tau)\mathbf{w}_{k^c} + \tilde{A}^c(\tau)\mathbf{w}_{-k^c}$$

for some $k^c \in S$. Here, the amplitude function $\tilde{A}(\tau)$ satisfies the following S-L equation:

$$\frac{d\tilde{A}}{d\tau} = \mu\tilde{\psi}\tilde{A} + \tilde{\phi}\tilde{A}^3. \tag{17}$$

The details regarding the derivation of (17) and explicit expressions for the parameters $\tilde{\phi}$ and $\tilde{\psi}$ are given in Appendix A.2. Since coefficients of S-L equation (17) are real, the amplitude $\tilde{A}$ takes real values.

Steady state solutions of the equation (17) are also given by

$$\tilde{A}_0 = 0 \text{ and } \tilde{A}_\infty^\pm = \pm\sqrt{-\mu\tilde{\psi}/\tilde{\phi}}. \tag{18}$$

Similarly, we can conclude that the steady state solution $\tilde{A}_0$ (or $\mathbf{e}$) is unstable for $\mu = -1$ and stable for $\mu = 1$. This result is in consistence with the results of the linear analysis in Section 3. If $\tilde{\phi} < 0$, $\tilde{A}_\infty^\pm$ takes real values for $\mu = -1$. Thus we have the following result to approximate the stationary patterns arising from the CML.

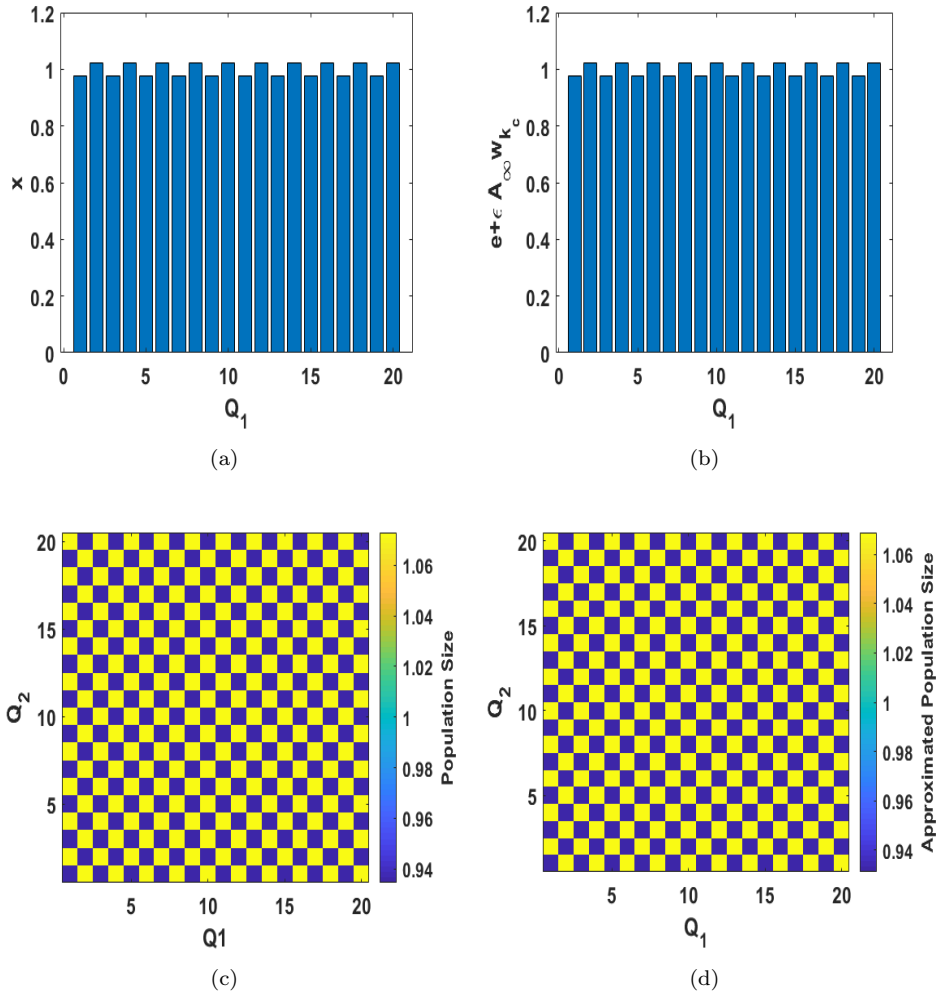

FIGURE 3. Comparison between numerical solutions to the CML (on the left) for examples **E1** and **E3**, and the weakly nonlinear first-order approximations of these solutions (on the right). Panel (a) illustrates stationary waves in a 1-dimensional habitat for **E1**. Similarly, panel (c) shows stationary patterns in a 2-dimensional habitat for **E3**. In panels (c) and (d), colors represent the population size and approximated population size, respectively.

Theorem 5.2. *Suppose that $\mu = -1$ and $\varepsilon > 0$ is small enough so that the uniform steady-state $\mathbf{e}$ is unstable to modes corresponding only to the eigenvalues k^c and $-k^c$. If $\tilde{\phi} < 0$, an approximation to the emerging solution to CML is given as follows:*

$$\mathbf{x} = \mathbf{e} + \varepsilon \tilde{A}_{\infty}^{\pm} \left(\mathbf{w}_{k^c} + \mathbf{w}_{-k^c} \right) + O(\varepsilon^2)$$

where $\tilde{A}_{\infty}^{\pm}$ are as in (18).

For the parameters and kernels described in example **E2**, we have two eigenvalues that are complex conjugates of each other. A solution to the CML with these parameters and a random initial datum is given in Panel (a) of Figure 4 and an approximation to this solution is shown in Panel (b) of Figure 4. Here $\varepsilon = 0.0079$ and it is also verified that the error in predicting the amplitude is of order ε^2. In addition, the equilibria of the S-L equation are given by $A_\infty^\pm = \pm 6.3505$. The maximum norm of the difference between the stationary solution and its approximation is given by $\|\mathbf{x} - \mathbf{e} - \varepsilon A_\infty^+(\mathbf{w}_{k_1^c} + \mathbf{w}_{k_2^c})\|_\infty = 0.0102$, where $k_1^c = 6$ and $k_2^c = 14$.

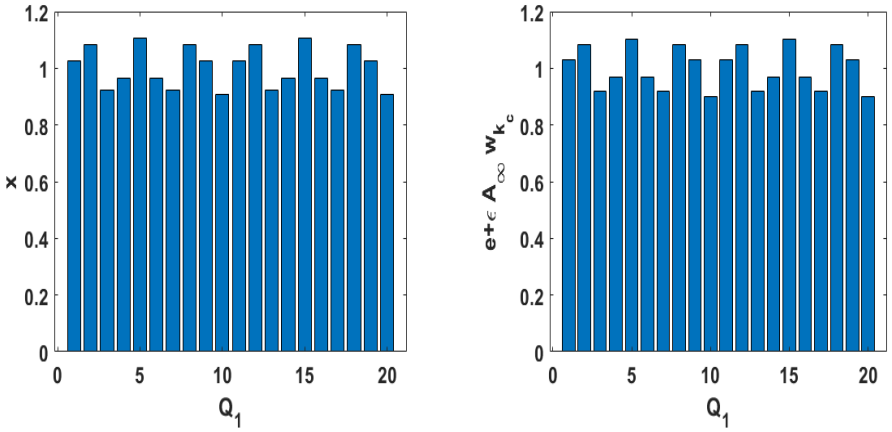

(a) (b)

FIGURE 4. Comparison between numerical solutions to CML (on the left) and the weakly nonlinear first order approximation of these solutions (on the right). Panel (a) illustrates stationary waves in a 1-dimensional habitat for the parameters given in example **E2**.

5.2. **Stuart-Landau equations for two amplitude functions.** As in the example **E4**, there may be two eigenvalues that are not the complex conjugates of each other. In this case we have

$$\mathbf{x}_1 = A_1(\tau)\mathbf{w}_{k_1^c} + A_2(\tau)\mathbf{w}_{k_2^c}$$

for some $k_1^c, k_2^c \in S$. These amplitude functions A_1 and A_2 satisfy the following system of S-L equations:

$$\begin{aligned} \frac{dA_1}{d\tau} &= \phi_1 A_1^3 + \xi_1 A_1 A_2^2 + \mu\psi_1 A_1 \\ \frac{dA_2}{d\tau} &= \phi_2 A_2^3 + \xi_2 A_1^2 A_2 + \mu\psi_2 A_2 \end{aligned} \tag{19}$$

The details regarding the derivation of the system of S-L equations and explicit expressions for its parameters are given in Appendix A.3. Here we would like to

note that nontrivial stationary solutions to (19) are given in [17] as follows:

$$P_1^{\pm} = \Big(\pm \sqrt{-\mu\psi_1/\phi_1}, 0\Big);\ P_2^{\pm} = \Big(0, \pm\sqrt{-\mu\psi_2/\phi_2}\Big)$$

$$P_3^{(\pm,\pm)} = \left(\pm\sqrt{\frac{\mu\psi_1(\xi_1-\phi_2)}{\phi_1\phi_2-\xi_1\xi_2}}, \pm\sqrt{\frac{\mu\psi_2(\xi_2-\phi_1)}{\phi_1\phi_2-\xi_1\xi_2}} \right)$$

To approximate the stationary patterns arising from the CML, we have the following result:

Theorem 5.3. *Suppose that $\mu = -1$ and $\varepsilon > 0$ is small enough so that the uniform steady-state $\mathbf{e}$ is unstable to modes corresponding only to the eigenvalues k_1^c and k_2^c. An approximation to the emerging solution to CML is given as follows:*

$$\mathbf{x} = \mathbf{e} + \varepsilon\big(A_{1\infty}\mathbf{w}_{k_1^c} + A_{2\infty}\mathbf{w}_{k_2^c}\big) + O(\varepsilon^2)$$

where $(A_{1\infty}, A_{2\infty})$ is a stationary state of the Stuart-Landau equation (19).

For **E4**, we have two eigenvalues that are not complex conjugates of each other. Hence, one needs to consider two different amplitude functions A_1 and A_2. A solution to the CML with a random initial datum and its predicted equilibrium solution to first order are shown in Panels (a) and (b) of Figure 5, respectively. Here $\varepsilon = 0.0154$ and it is also verified that the error in predicting the amplitude is of order ε^2. Since the S-L equation (19) is symmetric in A_1 and A_2, we take only $P_3^{(\pm,\pm)}$ into consideration when calculating the approximation. Then we have $P_3^{(\pm,\pm)} = (\pm 7.5993, \pm 7.5993)$. The maximum norm of the difference between the stationary solution and its approximation is then given by $\|\mathbf{x}-\mathbf{e}-\varepsilon A_{1\infty}\mathbf{w}_{k_1^c} - \varepsilon A_{2\infty}\mathbf{w}_{k_2^c})\|_\infty = 0.0385$, where $k_1^c = (10, 20)$, $k_2^c = (20, 10)$ and $A_{1\infty} = A_{2\infty} = 7.5993$.

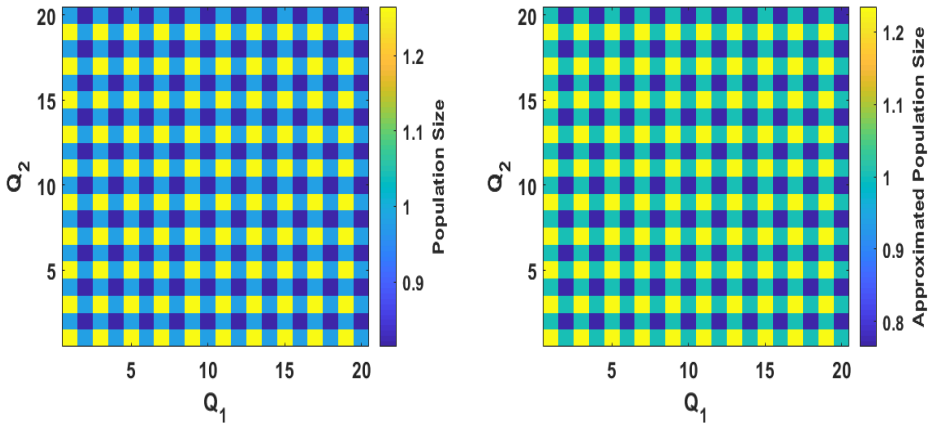

(a) (b)

FIGURE 5. Comparison between numerical solution to CML (on the left) and the weakly nonlinear first order approximation of this solutions (on the right). Panel (a) illustrates stationary waves in a 2-dimensional habitat for **E4**. In panels (a) and (b), colors represent the population size and approximated population size, respectively.

6. **Conclusion.** In this paper, we studied the stationary patterns arising from a discrete-time metapopulation model with nonlocal competition. Our model is a generalization of the metapopulation dynamics with quasi-local competition introduced in [11]. We have investigated the pattern formation mechanism induced by nonlocal competition in 1-D and 2-D spatial domains.

The single-species model studied in this paper belongs to a large family of spatial models taking nonlocal interactions into account. In the literature, there are continuous-time and space [2, 7, 14, 15, 18, 37], continuous-time and discrete space [4, 30] and continuous space and discrete-time [5] intraspecific competition models studying the effects of nonlocal interactions on the stability of the space-homogeneous solution. In all of the above-mentioned works, it was shown that nonlocal interactions destabilize the space-homogenous solution if the Fourier transform of the competition kernel takes negative values for some wavenumbers. We argued that the CML model studied in this paper is no exception by showing that $\mathbf{e}$ becomes unstable when the Fourier transform of the competition kernel takes negative values. In addition, as discussed in Section 3, this is a general condition on the destabilization of the steady-state which agrees with the result obtained in [11].

We further analyzed the model by obtaining the Stuart-Landau (S-L) equations providing a mathematical description of the CML close to the onset of instability. To the best of our knowledge, this is the first study performing a weakly nonlinear analysis on a CML model in the literature. The S-L equations have been used to approximate the stationary patterns arising from the model in 1-D and 2-D habitats. We numerically verified the results of nonlinear analysis. The result of weakly nonlinear analysis implies that as the dispersal rate δ decreases, the amplitude levels of patterns increase and are of order $\varepsilon = \sqrt{\delta_0 - \delta}$. Hence, we conclude that the smaller dispersal rate favors aggregation. This result is in line with the findings presented in [2, 3, 7, 18]

Instead of assuming nearest-neighbor interactions, we assumed that the strength of the ecological interactions (including dispersal) impinging on a population in a patch is a function of the neighboring population densities as well as of their spatial distance, with more distant patches having a smaller impact. Assuming nonlocal rather than quasi-local interactions leads to the emergence of more complex spatial patterns as shown in Figure 4.

Future analysis might move from stationary patterns to traveling patterning waves and obtaining S-L equations for traveling wave type patterns. In this case, the corresponding S-L equations will have complex coefficients. In addition, weakly nonlinear analysis for a single species CML model can be extended to analyze dispersal driven instabilities in two or more species discrete-in-time and -space equations (see, e.g., [36]).

Appendix A. Weakly nonlinear analysis.

A.1. **When there is a simple eigenvalue.** In this case, we have $\mathbf{x}_1 = A(\tau)\mathbf{w}_{k^c}$ for some $k^c \in S$. Note that for both examples the critical eigenvalue $\mathbf{w}_{k^c}$ couples only with the eigenvalue $\mathbf{w}_0 = 1$. Thus the second order solution is of the form $\mathbf{x}_2 = B(\tau)\mathbf{w}_0$.

Substituting (13) into the full system (5) and using (14), the following sequence of equations can be obtained.

At $O(1)$,we have $\mathbf{e} = \mathbf{e}$. At the level $O(\varepsilon)$, one gets the linear relationship (9) as follows:

$$1 = (\delta_0(D_{k^c} - 1) + 1)(C_{k^c} + \lambda - C_{k^c}\lambda)/\lambda.$$

At $O(\varepsilon^2)$, we obtain:

$$\lambda B - \lambda^2 B - aA^2 C_{k^c}(C_{k^c} + \lambda - C_{k^c}\lambda) = 0.$$

From the last equality we obtain:

$$B = aA^2 C_{k^c} \frac{C_{k^c} + \lambda - C_{k^c}\lambda}{\lambda(1-\lambda)}$$

At level $O(\varepsilon^3)$, we obtain the S-L equation (15) with parameters

$$\phi = a^2 C_{k^c} \frac{(\delta_0 \hat{D}_{k^c} - \delta_0 + 1)\big((1-\lambda)C_{k^c}^2 - C_{k^c}\lambda^2 + 2\hat{C}_{k^c}\lambda + \lambda^2\big)}{\lambda^3(\lambda - 1)} \tag{20}$$

and

$$\psi = \lambda^{-1}(D_{k^c} - 1)(C_{k^c} + \lambda - C_{k^c}\lambda). \tag{21}$$

A.2. **When there are a pair of complex conjugate eigenvalues.** Note that the eigenvector $\mathbf{w}_{k^c}$ (where $k^c = 6$) and its complex conjugate couple only with the eigenvalues $\mathbf{w}_0, \mathbf{w}_{2k^c}$. and $\mathbf{w}_{-2k^c}$.Thus the second-order solution is of the form $\mathbf{x}_2 = B_0(\tau)\mathbf{w}_0 + B_1(\tau)\mathbf{w}_{2k^c} + B_1^c(\tau)\mathbf{w}_{-2k^c}$. At level $O(\varepsilon)$ one gets the linear relationship for each eigenvector.

Similarly one obtains the following equalities at level $O(\varepsilon^2)$:

$$\begin{aligned} B_0 &= \beta_0 \tilde{A}^2 \\ B_1 &= \beta_1 \tilde{A}^2, \end{aligned}$$

where

$$\begin{aligned} \beta_0 &= 2a\frac{C_{k^c} + \lambda - \lambda C_{k^c}}{\lambda - \lambda^2}, \\ \beta_1 &= aC_{k^c}\frac{(C_{k^c} + \lambda - \lambda C_{k^c})(D_{2k^c}\delta_0 - \delta_0 + 1)}{\lambda(C_{2k^c} + \lambda - \lambda C_{2k^c})(\delta_0 + \lambda - D_{2k^c}\delta_0 - 1) - \lambda^2}, \end{aligned}$$

At level $O(\varepsilon^3)$, we obtain the S-L equation (17) with parameters

$$\begin{aligned} \tilde{\phi} &= -a\lambda^{-3}(D_{k^c}\delta_0 - \delta_0 + 1)\big((2C_{k^c} - C_{k^c}\lambda + \lambda)\lambda\beta_0 + \\ &\quad +(C_{k^c}\lambda + C_{2k^c}\lambda + 2C_{k^c}C_{2k^c} - 2C_{k^c}C_{2k^c}\lambda)\lambda\beta_1 + 3C_{k^c}^2 a(C_{k^c}\lambda - \lambda - C_{k^c})\big), \\ \tilde{\psi} &= \lambda^{-1}(D_{k^c} - 1)(C_{k^c} + \lambda - \lambda C_{k^c}), \end{aligned} \tag{22}$$

A.3. **When there are two amplitude functions.** Note that the eigenvalue $\mathbf{w}_{k_i^c}$ (where $k_1^c = (0, 10)$ and $k_2^c = (10, 0)$) couple only with the eigenvalues $\mathbf{w}_{0,0}$ and $w_{10,10}$. Thus the second order solution is of the form $\mathbf{x}_2 = B_0(\tau)\mathbf{w}_{0,0} + B_1(\tau)\mathbf{w}_{10,10}$. At level $O(\varepsilon)$one gets the linear relationship for each eigenvector. Similarly one obtains the following equalities at level $O(\varepsilon^2)$:

$$\begin{aligned} B_0 &= \beta_1 A_1^2 + \beta_2 A_2^2 \\ B_1 &= \beta_3 A_1 A_2 \end{aligned}$$

where

$$\begin{aligned}
\beta_1 &= a\frac{C_{k_1^c}(C_{k_1^c}+\lambda-C_{k_1^c}\lambda)}{\lambda(1-\lambda)},\\
\beta_2 &= a\frac{C_{k_2^c}(C_{k_2^c}+\lambda-C_{k_2^c}\lambda)}{\lambda(1-\lambda)},\\
\beta_3 &= a\frac{(\delta_0 D_{k_1^c+k_2^c}-\delta_0+1)\big(\lambda(C_{k_1^c}+C_{k_2^c})+2C_{k_1^c}C_{k_2^c}(1-\lambda)\big)}{\lambda(C_{k_1^c+k_2^c}+\lambda-\lambda C_{k_1^c+k_2^c})(D_{k_1^c+k_2^c}\delta_0-\delta_0+1)-\lambda^2}.
\end{aligned}$$

Eventually we obtain system of differential equations (19) at level $O(\varepsilon^3)$ with the following parameters:

$$\begin{aligned}
\phi_1 &= \lambda^{-3}a(D_1\delta_0-\delta_0+1)\Big(aC_{k_1^c}^2(C_{k_1^c}+\lambda-C_{k_1^c}\lambda)+\beta_1\lambda(C_{k_1^c}\lambda-2C_{k_1^c}-\lambda)\Big)\\
\xi_1 &= -\lambda^{-3}a(D_{k_1^c}\delta_0-\delta_0+1)\Big(\big(\beta_2(1-C_{k_1^c})+\beta_3(C_{k_2^c}+C_{k_1^c+k_2^c}-2C_{k_2^c}C_{k_1^c+k_2^c})\big)\lambda^2+\\
&\quad+\big(2\beta_2C_{k_1^c}+2\beta_3C_{k_2^c}C_{k_1^c+k_2^c}+aC_{k_2^c}(3C_{k_1^c}C_{k_2^c}-C_{k_2^c}-2C_{k_1^c})\big)\lambda-3aC_{k_1^c}C_{k_2^c}^2\Big)\\
\psi_1 &= \lambda^{-1}(D_{k_1^c}-1)(C_{k_1^c}+\lambda-C_{k_1^c}\lambda)\\
\phi_2 &= \lambda^{-3}a(D_{k_2^c}\delta_0-\delta_0+1)\Big(aC_{k_2^c}^2(C_{k_2^c}+\lambda-C_{k_2^c}\lambda)+\beta_2\lambda(C_{k_2^c}\lambda-2C_{k_2^c}-\lambda)\big)\\
\xi_2 &= -\lambda^{-3}a*(D_{k_2^c}\delta_0-\delta_0+1)\Big(\big(\beta_1(1-C_{k_2^c})+\beta_3(C_{k_1^c}+C_{k_1^c+k_2^c}-2C_{k_1^c}C_{k_1^c+k_2^c})\lambda^2+\\
&\quad+\big(2\beta_1C_{k_2^c}+2\beta_3C_{k_1^c}C_{k1^c+k_2^c}+aC_{k_1^c}(3C_{k_1^c}C_{k_2^c}-C_{k_1^c}-2C_{k_2^c})\big)\lambda-3aC_{k_1^c}^2C_{k_2^c}\Big)\\
\psi_2 &= \lambda^{-1}(D_{k_2^c}-1)(C_{k_2^c}+\lambda-C_{k_2^c}\lambda)
\end{aligned}$$

REFERENCES

[1] L. J. Allen, Y. Lou and A. L. Nevai, Spatial patterns in a discrete-time SIS patch model, *J. Math. Biol.*, **58**, (2009), 339–375.

[2] O. Aydogmus, Patterns and transitions to instability in an intraspecific competition model with nonlocal diffusion and interaction, *Math. Modell. Nat. Phenom.*, **10** (2015), 17–29.

[3] O. Aydogmus, Discovering the effect of nonlocal payoff calculation on the stabilty of ess: Spatial patterns of hawk–dove game in metapopulations, *J. Theor. Biol.*, **442** (2018), 87–97.

[4] O. Aydogmus, Phase transitions in a logistic metapopulation model with nonlocal interactions, *Bull. Math. Biol.*, **80** (2018), 228–253.

[5] O. Aydogmus, Y. Kang, M. E. Kavgaci and H. Bereketoglu Dynamical effects of nonlocal interactions in discrete-time growth-dispersal models with logistic-type nonlinearities, *Ecol. Complexity*, **31** (2017), 88–95.

[6] M. Beekman, D. Sumpter and F. Ratnieks Phase transition between disordered and ordered foraging in pharaoh's ants, *Proc. Natl. Acad. Sci. U.S.A*, **98** (2015), 9703–9706.

[7] N. Britton, Aggregation and the competitive exclusion principle, *J. Theor. Biol.*, **136** (1989), 57–66.

[8] R. Cantrell and C. Cosner, *Spatial Ecology via Reaction-Diffusion Equations*, John Wiley & Sons, 2003.

[9] C. Cobbold, F. Lutscher and J. Sherratt, Diffusion-driven instabilities and emerging spatial patterns in patchy landscapes, *Ecol. Complexity*, **24** (2015), 69–81.

[10] N. B. Davies, *Dunnock Behaviour and Social Evolution*, 3, Oxford University Press, 1992.

[11] M. Doebeli and T. Killingback, Metapopulation dynamics with quasi-local competition, *Theor. Popul. Biol.*, **64** (2003), 397–416.

[12] R. Durrett and S. Levin, The importance of being discrete (and spatial), *Theor. Popul. Biol.*, **46** (1994), 363–394.

[13] R. Eftimie, G. de Vries and M. Lewis, Weakly nonlinear analysis of a hyperbolic model for animal group formation, *J. Math. Biol.*, **59** (2009), 37–74.

[14] M. Fuentes, M. Kuperman and V. Kenkre, Nonlocal interaction effects on pattern formation in population dynamics, *Phys. Rev. Lett.*, **91** (2003), 158104.

[15] M. Fuentes, M. Kuperman and V. Kenkre, Analytical considerations in the study of spatial patterns arising from nonlocal interaction effects, *J. Phys. Chem. B*, **108** (2004), 10505–10508.
[16] G. Gambino, M. C. Lombardo and M. Sammartino, Turing instability and traveling fronts for a nonlinear reaction–diffusion system with cross-diffusion, *Math. Comput. Simul.*, **82** (2012), 1112–1132.
[17] G. Gambino, M. C. Lombardo and M. Sammartino, Pattern formation driven by cross-diffusion in a 2d domain, *Nonlinear Anal. Real World Appl.*, **14** (2013), 1755–1779.
[18] S. Genieys, V. Volpert and P. Auger, Pattern and waves for a model in population dynamics with nonlocal consumption of resources, *Math. Modell. Nat. Phenom.*, **1** (2006), 63–80.
[19] M. Gilpin and I. Hanski, *Metapopulation Biology: Ecology, Genetics, and Evolution*, Academic Press, 1997.
[20] M. Gyllenberg, G. Söderbacka and S. Ericsson, Does migration stabilize local population dynamics? Analysis of a discrete metapopulation model, *Math. Biosci.*, **118** (1993), 25–49.
[21] I. Hanski, A practical model of metapopulation dynamics, *J. Anim. Ecol.*, (1994), 151–162.
[22] J. von Hardenberg, E. Meron, M. Shachak and Y. Zarmi, Diversity of vegetation patterns and desertification, *Phys. Rev. Lett.*, **87** (2001), 198101.
[23] M. P. Hassell, N. H. Comins and R. M. May, Spatial structure and chaos in insect population dynamics, *Nature* **353**, (1991) 255–258.
[24] M. H. Holmes, *Introduction to Perturbation Methods*, 20, Springer Science & Business Media, 2012.
[25] R. Lefever and O. Lejeune, On the origin of tiger bush, *Bull. Math. Biol.*, **59** (1997), 263–294.
[26] S. Levin, Dispersion and population interactions, *Am. Nat.*, (1974), 207–228.
[27] R. Levins, Extinction, in *Some Mathematical Questions in Biology*, American Mathematical Society, Providence, RI.
[28] Y. Lou, W.-M. Ni and S. Yotsutani, Pattern formation in a cross-diffusion system, *Discrete Contin. Dyn. Syst.*, **35** (2015), 1589–1607.
[29] F. Lutscher, *Integrodifference Equations in Spatial Ecology*, Springer International Publishing, 2019.
[30] N. Madras, J. Wu and X. Zou, Local-nonlocal interaction and spatial-temporal patterns in single species population over a patchy environment, *Canad. Appl. Math. Q.*, **4** (1996), 109–133.
[31] M. Mandal and A. Asif, *Continuous and Discrete Time Signals and Systems*, Cambridge University Press, 2007.
[32] Y. E. Maruvka and N. M. Shnerb, Nonlocal competition and logistic growth: Patterns, defects, and fronts, *Phys. Rev. E*, **73** (2006), 011903.
[33] J. Murray, *Mathematical biology ii: Spatial models and biomedical applications*, Springer, 2003.
[34] M. Neubert, M. Kot and M. Lewis, Dispersal and pattern formation in a discrete-time predator-prey model, *Theor. Pop. Biol.*, **48** (1995), 7–43.
[35] A. Okubo and S. Levin, *Diffusion and Ecological Problems: Modern Perspectives*, 14, Springer Science & Business Media, 2013.
[36] L. A. D. Rodrigues, D. C. Mistro and S. Petrovskii, Pattern formation in a space-and time-discrete predator–prey system with a strong allee effect, *Theor. Ecol.*, **5** (2012), 341–362.
[37] A. Sasaki, Clumped distribution by neighbourhood competition, *J. Theor. Biol.*, **186** (1997), 415–430.
[38] J. Smith, *Mathematics of the Discrete Fourier Transform (DFT): With Audio Applicaitons*, W3K Publishing, 2007.
[39] J. Stuart, On the non-linear mechanism of wave disturbances in stable and unstable parallel flows. part i, *J. Fluid Mech.*, **9** (1960), 152–171.
[40] C. Topaz, A. Bertozzi and M. Lewis, A nonlocal continuum model for biological aggregation, *Bull. Math. Biol.*, **68** (2006), 1601–1623.
[41] A. Turing, The chemical basis of morphogenesis, *Philos. Trans. R. Soc. London, Ser. B.*, **237** (1952), 37–72.

Received October 2020; 1st revision April 2021; 2nd revision May 2021.

E-mail address: ozgur.aydogmus@asbu.edu.tr
E-mail address: yun.kang@asu.edu